

# ON FEATURE EXTRACTION FOR TEXTURE ANALYSIS

Csaba István KISS\*, Géza NÉMETH\*, Dmitrij CHETVERIKOV\*\* and  
Lilla BÖRÖCZKY\*\*

\* KFKI Research Institute for Measurement and Computing Techniques  
P. O. Box 49, H-1525 Budapest, Hungary

\*\* Computer and Automation Research Institute of Hungarian Academy of Sciences  
P. O. Box 63, H-1518 Budapest, Hungary

Received: June 30, 1995

## Abstract

Texture analysis has a fundamental importance in image processing and it is widely applied for different fields, e.g. industrial quality control, biomedical imagery, etc. For each texture classification/segmentation problem feature extraction is a crucial task. In this paper we review several methods of feature extraction, such as statistical approaches, transform-based methods and pixel-based structural descriptions. Beside of their principles, advantages and disadvantages occurring during their applications are also described. Theoretical and experimental investigations showed that multichannel texture analysis is an efficient tool and has several advantages with respect to the traditional feature extraction methods. Pixel-based structural features are also presented, which attempt to bridge the gap between statistical and structural feature extraction methods.

*Keywords:* texture, texture analysis, feature extraction, segmentation, classification, quality control.

## 1. Introduction

Texture analysis plays an important role in computer vision and pattern recognition as well as in image processing and it is widely applied to many areas, e.g. analysis of satellite images, industrial quality control, biomedical imagery, remote sensing, etc.

The process of texture discrimination can be divided into three phases, such as feature extraction, feature selection and classification/segmentation. Extraction of texture features deals with the computation of features from the image data, which completely embody information on the spatial distribution of gray level variation in the texture. Generally, a set of features is used for texture discrimination, however, no definite conclusion which set of features has the best overall performance.

The subject of feature selection in texture analysis is concerned with mathematical tools to create the optimal feature set characterising sufficiently the distinguishing properties of the different texture classes.

In this paper we will focus on the feature extraction, that is to compute the features from a textured image. Most existing texture features and the texture analysis itself can be divided into two categories, namely structural and statistical ones. The former approach is based on the view that textures are made up of primitives appearing in more or less regular repetitive spatial arrangements. They are appropriate for periodic textures with low noise, however, those are seldom encountered in real-applications. The use of statistical features is motivated by the human discrimination of textures [1], that human beings are sensitive to the second-order statistics. The statistical feature extraction techniques are mainly of three types: spatial gray level dependence methods [2–4], stochastic model-based features [3–5], and transform/filtering methods [6, 14, 34].

First, feature extraction based on statistical methods will be discussed in Section 2. In Section 3 the transform-based methods, such as Gabor filtering and wavelet decomposition applied for texture analysis are presented. Several pixel-based structural features, e.g. texture regularity, anisotropy and symmetry are discussed in Section 4. Finally, a conclusion and main topics of the future research will be given.

## 2. Spatial Gray Level Dependence Methods

The most popular spatial gray level dependence methods [5] are based on the cooccurrence, run length and statistical feature matrices, which will be discussed below. Suppose the area to be analysed for texture is rectangular and has  $N_c$  pixels in the horizontal direction,  $N_r$  pixels in the vertical direction, and the gray tone of each pixel is quantized to  $N_g$  levels.

### 2.1 Cooccurrence Matrix

The gray tone cooccurrence can be specified in a matrix of relative frequencies  $P_{ij}$  with which two pixels separated by distance  $d$  and orientation  $\varphi$  occurs on the image, one with gray tone  $i$  and the other with gray tone  $j$  [5].

The cooccurrence matrices are symmetric and they are functions of the angular relationship between neighbouring pixels as well as functions of the distance between them. Consider *Fig. 1*, which represents a  $4 \times 4$  image with four gray tones ranging from 0 to 3.

In this example the operator  $P(i, j)$  denotes the number of pairs  $(i, j)$ ,  $d = 1$  and  $\varphi = 0^\circ, 45^\circ, 90^\circ, 135^\circ$ .

From the cooccurrence matrices several features can be calculated for texture discrimination purposes. *Fig. 2* shows the most commonly used features [5].

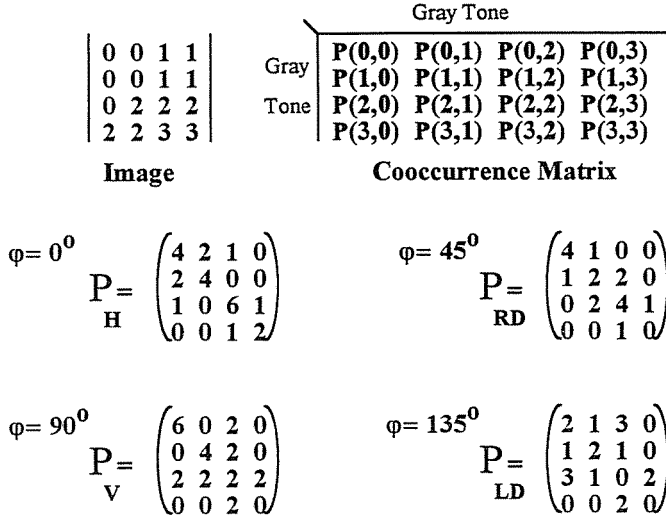


Fig. 1. The spatial cooccurrence calculation [5]

<i>Uniformity or Energy</i>	$F1 \equiv \sum_{i,j} P_{i,j}^2$
<i>Entropy</i>	$F2 \equiv \sum_{i,j} P_{i,j} \cdot \log P_{i,j}$
<i>Contrast</i>	$F3 \equiv \sum_{i,j} P_{i,j} \cdot  i - j ^k$
<i>Inverse difference moment</i>	$F4 \equiv \sum_{i,j} \frac{P_{i,j}}{ i - j ^k}, \quad i \neq j$
<i>Correlation</i>	$F5 \equiv \sum_{i,j} (i - u)(j - u) \frac{P_{i,j}}{\sigma^2}$

Fig. 2. Common features computed from the cooccurrence matrix

For a homogeneous texture the uniformity has relatively large values, because there are few dominant gray tone transitions in the image. How-

ever, the value of the contrast is large when the texture is a nonhomogeneous one. The correlation feature is a measure of gray tone linear dependencies in the image. Thus, this value will be considerably larger for such textures than for other cases.

## 2.2 Run Length Matrix

A gray level run is a set of consecutive, collinear picture points having the same gray level value. The length of the run is the number of pixels in the run.

For a given picture, a gray level run length matrix is computed for runs having any predefined direction. The matrix element  $(i, j)$  specifies the number of times that the picture contains a run of length  $j$  consisting of points having gray level  $i$ , in the given direction. Hence  $i$  can vary from zero to  $\{N_g - 1\}$  and  $j$  can go from one to the maximum of  $\{N_c$  or  $N_r\}$ .

Gray level runs can be characterised by the gray tone, the length and the direction of the run. GALLOWAY [3] used four main directions:  $0^\circ, 45^\circ, 90^\circ, 135^\circ$ , and for each direction she computed the joint probability of gray tone of run and the run length.

The example of *Fig. 3* shows a  $4 \times 4$  picture having four gray levels (0,1,2,3), and the resulting run length matrices for the four principal directions.

To obtain numerical texture measures from the matrices, we can compute functions analogous to cooccurrence matrices. Let  $N_l$  be the number of different run length occur and *Fig. 4* shows five main features.

In the first feature the run length values are divided by the square of the length of the run  $j^2$ , thus it emphasises short runs. The second feature is similar to the first one, but it characterises the long runs by multiplying each run length value by  $j^2$ .

The gray level nonuniformity squares the number of the run lengths for each gray level. In the texture where runs are equally distributed throughout the gray levels, this measure takes on its lowest value. If the runs are equally distributed throughout the length, the run length nonuniformity will have a low value. Run percentage should have its lowest value for textures with the most linear structure.

## 2.3 Statistical Feature Matrix

WU and CHEN [4] have proposed a new texture feature extraction technique using statistical feature matrices (SFM). The most commonly used second-order statistical features in the spatial gray level dependence meth-

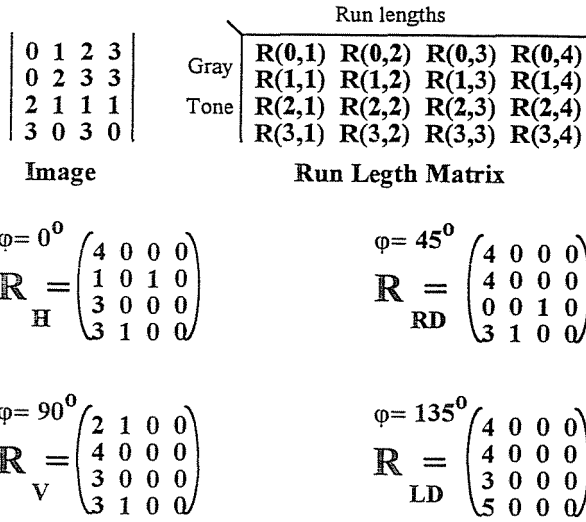


Fig. 3. The run length matrix calculation

<i>Short runs emphasis</i>	$E1 \equiv \sum_{i=0}^{Ng-1} \sum_{j=1}^{Nl} \frac{R(i, j)}{j^2} \bigg/ \sum_{i=0}^{Ng-1} \sum_{j=1}^{Nl} R(i, j)$
<i>Long runs emphasis</i>	$E2 \equiv \sum_{i=0}^{Ng-1} \sum_{j=1}^{Nl} j^2 R(i, j) \bigg/ \sum_{i=0}^{Ng-1} \sum_{j=1}^{Nl} R(i, j)$
<i>Gray-level nonuniformity</i>	$E3 \equiv \sum_{i=0}^{Ng-1} \left( \sum_{j=1}^{Nl} R(i, j) \right)^2 \bigg/ \sum_{i=0}^{Ng-1} \sum_{j=1}^{Nl} R(i, j)$
<i>Run length nonuniformity</i>	$E4 \equiv \sum_{j=1}^{Nl} \left( \sum_{i=0}^{Ng-1} R(i, j) \right)^2 \bigg/ \sum_{i=0}^{Ng-1} \sum_{j=1}^{Nl} R(i, j)$
<i>Run percentage</i>	$E5 \equiv \sum_{i=0}^{Ng-1} \sum_{j=1}^{Nl} R(i, j) \bigg/ \sum_{i=0}^{Ng-1} \sum_{j=1}^{Nl} j \cdot R(i, j)$

Fig. 4. Features computed from the run length matrix

ods are contrast, covariance and dissimilarity. The statistical feature matrices evaluate directly these three statistical features for several intersamples spacing distances from the image instead of indirectly estimating them e.g. from cooccurrence or run length matrices.

Let  $S = \{x, y\}$  be the spatial coordinates of an  $L_y \times L_x$  array of pixels and  $I(x, y)$  be the intensity at a pixel. Definitions of these features are:

$$\begin{aligned} \delta \text{ Contrast} & \quad \text{CON}(\delta) \equiv E\{[I(x, y) - I(x + \Delta x, y + \Delta y)]^2\} \\ \delta \text{ Covariance} & \quad \text{COV}(\delta) \equiv E\{[I(x, y) - \eta][I(x + \Delta x, y + \Delta y) - \eta]\} \\ \delta \text{ Dissimilarity} & \quad \text{DSS}(\delta) \equiv E\{|I(x, y) - I(x + \Delta x, y + \Delta y)|\} \end{aligned}$$

where:  $E\{\cdot\}$  denotes the expectation operation;

$\delta = (\Delta x, \Delta y)$  represents the intersample spacing distance vector;

$\eta$  is the average gray level of an image.

Other  $\delta$  statistical features may also be defined in the same way.

On the basis of the previous definitions, the statistical feature matrix can be defined as follows.

**SFM** (Statistical Feature Matrix) is an  $(L_r + 1) \times (2L_c + 1)$  matrix whose  $(i, j)$  element is the  $\mathbf{d}$  statistical feature of an image. The  $\mathbf{d} = (j - L_c, i)$  is an intersample spacing distance vector for  $i = 0, 1, \dots, L_r$ ,  $j = 0, 1, \dots, 2L_c$  and  $L_r, L_c$  are the constants that determine the maximum intersample spacing distance. Examples are the contrast matrix ( $\mathbf{M}_{\text{con}}$ ), covariance matrix ( $\mathbf{M}_{\text{cov}}$ ), and dissimilarity matrix ( $\mathbf{M}_{\text{dss}}$ ) of the image that can be defined as the matrices whose  $(i, j)$  elements are the  $\mathbf{d}$  contrast,  $\mathbf{d}$  covariance,  $\mathbf{d}$  dissimilarity, respectively.

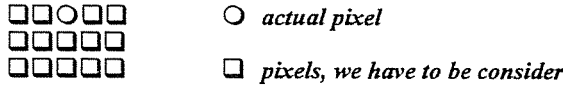
Fig. 5 shows an example for **SFM**. Let  $L_r = L_c = 2$ , so **SFM** is a  $3 \times 5$  matrix, where  $F[d(x, y)]$  is a particular feature computed for a given image with the intersample sampling vector  $\mathbf{d}$ .

Various values of  $L_r$  and  $L_c$  were chosen for different applications. They can be set to be  $L_x$  and  $L_y$ , respectively, for visual perceptual feature extraction, while small values are assigned to them for texture classification ( $L_r, L_c < 10$ ) [4].

### 3. Transform-Based Feature Extraction

Conventional feature extraction methods for texture analysis mainly focus on extracting gray level dependencies between image pixels on a single resolution. Probably the main difficulty of traditional texture analysis is the lack of appropriate tools to characterise effectively different resolutions of textures.

This problem can be overcome by multiresolution image analysis based on wavelet transform. First, as an introduction to wavelet theory,



**SFM:**

$$\begin{pmatrix} F[d(-2,0)] & F[d(-1,0)] & F[d(0,0)] & F[d(1,0)] & F[d(2,0)] \\ F[d(-2,1)] & F[d(-1,1)] & F[d(0,1)] & F[d(1,1)] & F[d(2,1)] \\ F[d(-2,2)] & F[d(-1,2)] & F[d(0,2)] & F[d(1,2)] & F[d(2,2)] \end{pmatrix}$$

*Fig. 5.* An example for SFM structure

we will discuss the Gabor transform, which is well-localised and well-concentrated in both time and frequency.

### 3.1 Gabor Transform

Time–frequency signal analysis can be carried out by expansion of the signal into a weighted sum of Gabor functions. The Gabor expansion of a 1D continuous signal  $f(t)$  is defined as

$$f(t) = \sum_{m=-\infty}^{+\infty} \sum_{n=-\infty}^{+\infty} G_{m,n} g_{m,n}(t),$$

$$g_{m,n}(t) = g(t - mT) e^{jn\Omega t}, \quad g(t) = e^{-\pi(t/T)^2},$$

where  $g_{m,n}(t)$  is called Gabor functions, which are the Gaussian-type functions,  $G_{m,n}$  are the Gabor coefficients [10] and  $T$  and  $\Omega$  represent the time and frequency sampling intervals, respectively.

Motivation of this decomposition mainly is due to the fact that Gabor functions have optimal localisation in the time and frequency as well. Unfortunately, there is no simple direct method for computing Gabor coefficients because the transform is not orthogonal. Furthermore, the numerical computations of the coefficients are very expensive and inefficient.

ORR [36] has proposed another method for computing Gabor coefficients based on Zak transform. Unfortunately, these algorithms could also lead to numerically troublesome expansions characterised by the fact that Gabor coefficients are not square summable.

In the two dimensional case, if the Gabor elementary functions are separable [37] similar results to the 1D case can be obtained. Since the energy in natural images is spread more or less uniformly within octave frequency bands and due to the 'octave-band division' feature of the human visual system, recursive pyramidal Gabor expansion was proposed in [37].

### 3.2 Wavelet Decomposition

Fourier transform has been the most useful technique for the frequency analysis of signals for long time. Due to the fact that sinusoids have an infinite support, such an approach has undesirable effects if one deals with signals which are localised in time and/or space. In the wavelet representation the basic functions can be generated from a single function by operations of dilation  $a$  and translation  $b$ :

$$\Psi_{a,b}(x) = a^{-1/2} \Psi \left( \frac{x-b}{a} \right).$$

The function  $\Psi(x)$  may be chosen depending on the application.

The wavelet representation

$$f(x) = \sum_{m=0}^{\infty} \sum_{n=0}^{\infty} c_n^m \cdot \Psi_{m,n}(x),$$

where

$$\Psi_{m,n}(x) = 2^{-m/2} \Psi(2^{-m}x - n)$$

has some important applications in image processing.

To construct function  $\Psi$ , we first determine a scaling function  $\Phi(x)$  which satisfies

$$\Phi(x) = \sqrt{2} \cdot \sum_k h_k \Phi(2x - k).$$

Then, function  $\Psi(x)$  will be

$$\Psi(x) = \sqrt{2} \cdot \sum_k g_k \Phi(2x - k),$$

where

$$g_k = (-1)^k h_{1-k}.$$

The forms of  $\Phi(x)$  and  $\Psi(x)$  are not required to perform the wavelet transform, which depends only on  $h_k$ . A  $J$  level decomposition

$$f(x) = \sum_k [c_{J+1,k} \Phi_{J+1,k}(x) + \sum_{j=0}^J d_{j,k} \Psi_{j+1,k}(x)]$$



can be given recursively. The coefficients  $c_{o,k}$  are given and for coefficients  $c_{j+1,n}$  and  $d_{j+1,n}$  the following relations hold:

$$c_{j+1,n} = \sum_k c_{j,k} \cdot h_{k-2n} ,$$

$$d_{j+1,n} = \sum_k c_{j,k} \cdot g_{k-2n} .$$

The numbers  $h_k$  can be found in [8].

This multiresolution wavelet transform results in a ‘compact’ non-redundant image representation in contrast to the traditional methods, such as low-pass filtering and Laplace pyramid transform [7].

For example, image decomposition by a 2D wavelet transform can be done as follows. The image is split into a low resolution part and the difference signal which describes the difference between the low resolution image and the actual one. Due to the correlation existing in the original image, the difference signal will have a histogram which is peaked around zero. The low resolution image still contains spatial correlations. Therefore, this decomposition can be repeated several times, so that a pyramidal image decomposition is created.

The size of a low level image is a quarter of the size of the original image. Hence, the number of coefficients needed to describe the difference is three times larger than the number of coefficients needed to describe the low resolution image. There are three different signals:  $d^{(1)}$ ,  $d^{(2)}$  and  $d^{(3)}$ .

$d^{(1)}$  indicates scale variations in the  $x$ -direction, and its high value indicates the presence of a vertical edge. Large values of  $d^{(2)}$  and  $d^{(3)}$  indicate the presence of a horizontal edge and a corner point, respectively (See *Fig. 6*).

ALDROUBI and UNSER [13] proposed a construction method of smooth wavelets, which tend to a Gabor function.

### 3.2.1. Feature Extraction Based on Wavelet Decomposition

Feature extraction based on wavelet transform has been studied by several authors. For texture analysis MALLAT [6] proposed a texture discrimination scheme based on discrete wavelet decomposition of textured images in order to obtain the fractal dimension of the particular textures. However, it is well known that the single fractal dimension is not sufficient to unique classification of different textures.

Another approach to feature extraction was developed by KUNDU et al. [12]. In this algorithm QMF filter bank was used to decompose

the texture into several subbands, and special features e.g. ‘zero-crossing’ features were calculated for the high-subbands.

Recently, CHANG and KUO proposed a quite efficient method [14]. Its main principle will be presented below: The idea of this approach leads to a new type of wavelet decomposition called tree-structured wavelet transform. The conventional multiresolution image representation based on wavelet transform decomposes subimages of the low frequency channels recursively. However, this decomposition is not very useful for a large class of natural textures because their most significant information appears in the middle frequency channels. For illustration, *Fig. 6* shows a traditional wavelet decomposition of texture ‘French Canvas’.

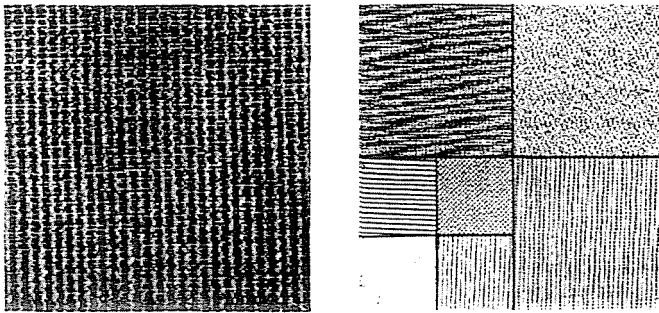


*Fig. 6.* Traditional wavelet decomposition of texture ‘French Canvas’

The key difference between this algorithm and the traditional pyramid wavelet representation is that the decomposition is no longer applied to the low frequency subsignals recursively. Instead, it can be applied to the different signals of each pyramid level. At first, a given texture image is decomposed into 4 subimages by a 2D wavelet transform. For all subimages an energy measure is calculated and compared with each other. If the energy of a subimage is significantly smaller than the others, we stop the decomposition in this region since it contains less information. The subimage containing higher energy will be decomposed further. This recursive and adaptive procedure can be represented by a quadtree structure or energy map.

For texture classification the feature set will be chosen from the energy map as the most dominant channel-energy values. It is worthwhile to note that the tree-structured wavelet transform is effective for textures which have dominant middle frequency channels. The application of the algorithm for different (nonperiodic, etc.) textures can be considered as a topic of future research.

## 4. High Level Texture Features

Statistical approaches apply a set of scalar features describing the distribution of intensities or local features. These methods usually pay less attention to the spatial interdependence in the image. The strength of statistical methods is in their robustness, relative simplicity and low computational cost.

Structural approaches concentrate on the spatial interaction of elementary regions, local features, or intensities. Next, several pixel-based structural approaches, such as regularity, anisotropy and symmetry, will be discussed.

### 4.1 Texture Regularity

The pixel-based structural approaches are often aimed at computing the dimensions of the periodicity parallelogram of a regular pattern. (See, for example, CONNERS and HARLOW [20] or ZUCKER and TERZOPOULOS [32].) Unfortunately, most of these methods fail to provide a meaningful description of both regular and random textures in the framework of a conceptually uniform model. Such a description should contain a measure of regularity which is interpretable in terms of global geometry (spatial arrangement), local geometry (shape and orientation of local features), and painting function (region intensity).

CONNERS and HARLOW [20] applied features computed on cooccurrence matrices (**CPM**), as a function of interpixel distance, to detect structure in natural textures. The entries of the cooccurrence matrix entries are the estimated probabilities of going from gray level  $i$  to gray level  $j$  given that the spacing is  $d$ . The moments are commonly used for texture description and classification. A regular pattern exhibits its periodicity through the moments plotted as a function of the spacing. Connors and Harlow applied periodicity analysis to the second moment of the **CPM**.

ZUCKER and TERZOPOULOS [32] applied the chi square test to cooccurrence matrices to find interpixel distances which yield matrices that capture maximally the regularity in a texture. The chi square approach was criticised by PARKKINEN et al. [30] who used another statistic. However, neither of the studies made an attempt to compare the regularity values of different textures.

MODESTINO et al. [29] considered a mosaic model for texture based on a rectangular partition of the plane by two mutually independent stationary renewal processes. The randomness parameter of the model provides a theoretical possibility of control of the mosaic randomness. However, this

parameter is omitted when a simplified version of the model is used to estimate the parameters of real-world textures.

Recently, ZHUANG and DUNN [31] have proposed the amplitude varying rate statistical approach for texture classification. Their method is based on the **Amplitude Varying Rate Matrix**. The elements of the **AVRM** are the frequencies of distances  $d$  occurring in a given direction between two pixels whose gray level is  $G$ .

Calculating AVRM amounts to computing the signed rate of change of intensity profiles for different values of the threshold (baseline). The value of the matrix depends on the neighbour relation between the baseline crossings. ZHUANG and DUNN [31] present an algorithm that computes an **AVRM** when neighbouring points are the nearest baseline crossings in a row.

The authors conclude that such a matrix contains information about the size of the texture primitives. To extract information on the placement of the primitives, the second nearest neighbour is taken. ZHUANG and DUNN [31] use the **AVRM** to compute a set of features for texture classification.

One of the features is introduced to indicate the degree of texture regularity. CHETVERIKOV [27] reports on an initial study that attempts to bridge the gap between random and regular texture analysers. A new approach is formulated based on a simple, well-parameterized one-dimensional stochastic process which enables one to generate the contrast curves of regular and random textures in a uniform way.

The generated curves are fitted to the experimental ones and three combinations of the parameters are defined which measure texture regularity. The proposed regularity measures are compared to the one introduced by ZHUANG and DUNN [31]. Experiments indicate that the regularity feature introduced by ZHUANG and DUNN [31] does not seem to be suitable for regularity analysis of natural textures.

However, it should be mentioned that the feature has been originally designed and used for texture classification rather than for regularity analysis. The contrast-based features proposed by Chetverikov were shown to measure regularity. An open question is whether they are useful for classification as well.

#### *4.2 Texture Anisotropy and Symmetry*

Since the publication of the recent stimulating paper by KASS and WITKIN [15] there has been growing interest in the investigation of oriented patterns such as texture images originating from flow-like processes. Directionality

has become a popular topic of texture research. (See e.g. [16-19].) Directionality can be viewed as local anisotropy that stems from dominating orientation of elongated texture elements. Computer analysis of this textural property usually involves orientation-sensitive filtering followed by local orientation coherence evaluation [15,16]. This can be done at variable scale.

JULESZ's pioneering work on preattentive (spontaneous) human texture perception (e.g. [33]) convinced the image analysis community that the second order statistics of texture images play a dominant role in spontaneous texture discrimination. This conjecture was supported by the impressive performance of the cooccurrence features in the computer analysis of texture patterns [30]. In many cases, similar features based on a simplified and faster version of the cooccurrence probability matrix (**CPM**) – the gray level difference histogram (**GLDH**) – were found [9,12] to yield as good results as the cooccurrence-based features.

Later the Julesz's conjecture was criticised as being applicable to limited classes of patterns. The interest of the researches has started to shift gradually towards attentive perception which is responsible for evaluation of fundamental properties as texture symmetry, directionality, regularity and structural complexity. In a recent paper [18], RAO and LOHSE reported on the results of a study of human texture perception aimed at identifying those high level texture features that account for most of the attentive texture discrimination capability of the human vision system.

They conclude that directionality and regularity are among the very few high level texture features that guide the process of perceptual grouping (taxonomy) of textural patterns.

Directionality is a special although perceptually important case of anisotropy. While this special case received considerable attention, anisotropy was studied in general in just a few early works on texture analysis. DAVIS [22] introduced the notion of cooccurrence-based polarogram. CHETVERIKOV used a more general term of anisotropy indicatrix (directional polar diagram) [9] and studied texture anisotropy via indicatrices depicting linear edge density and edge orientation distribution of texture edge map. Later, the anisotropy features introduced in [9] were successfully applied to rotation-invariant texture discrimination [11].

As it was pointed out in [9], the relevance of anisotropy analysis is to a large extent related to the crucial role played by symmetry in natural sciences in general and in human and computer vision in particular. Basic conservation laws of physics follow from the symmetry properties of the space-time. Analysis of a physical phenomenon (flow, field, etc.) is considerably simplified if a proper coordinate system is selected that complies with the symmetry (and anisotropy) of the phenomenon.

The same observation applies to texture patterns as well. JULESZ [33] concluded that the presence of symmetry facilitates human perception of texture. (For a recent short survey on the role of symmetry in vision, see [23].) KASS and WITKIN [15] emphasise correctly that directionality evaluation of oriented patterns is indispensable to properly set up the coordinate system for further detailed analysis.

Unfortunately, in many works on texture the patterns studied are manually pre-oriented so as to simplify the task in question. A more realistic case of arbitrary orientation and the problem of orientation sensitivity (compare to edge detection!) are rarely addressed. To approach these problems, one has to define axes of anisotropy (or, locally, axes of prevailing directionality [15]).

The increasing number of studies on symmetry of planar and 3D shapes and local gray-value patterns (see e.g. [24,25]) indicate the recognition of the role of symmetry in vision. Recently, a local symmetry operator has been applied to texture discrimination [26]. Motivated by this recognition as well as by the discovery of the importance of directionality for high level texture perception, CHETVERIKOV [27] reconsidered his previous research on anisotropy [11,12] in an attempt to use cooccurrence for detailed anisotropy analysis. He introduces the notion of extended GLDH and defines the GLDH features used to indicate anisotropy. In [12], examples of GLDH-based anisotropy indicatrices for random and regular textures are demonstrated and their stability under rotation shown.

Symmetry analysis of texture is done via anisotropy indicatrix and anisotropy axes are defined. Also, it is experimentally shown how indicatrices of a regular pattern vary with spacing magnitude. Finally, image resolution aspects of anisotropy are discussed.

## 5. Conclusions and Future Research

In this paper we review the methods of feature extraction, such as statistical approaches, transform-based methods and pixel-based structural descriptions for texture analysis. In the statistical feature extraction the principles of cooccurrence, run length and statistical feature matrix were outlined. In the transform-based approach Gabor filtering and the wavelet transform applied for feature extraction were discussed. Recent publications of this field show, that multichannel texture analysis is an efficient tool and has several advantages with respect to the traditional feature extraction methods. Several pixel-based structural features were also presented, which attempt to bridge the gap between statistical and structural feature extraction methods.

In future work we will focus on investigation of the wavelet transform in texture analysis more thoroughly, theoretically as well as experimentally. Furthermore, applications of other types of multiresolution approaches (biorthogonal wavelets, Gabor wavelets, etc.) for feature extraction are also planned. Design of complete texture classification/segmentation schemes for specific applications, e.g. for industrial quality control and biomedical imagery is also topic of our future research.

## References

1. JULESZ, B.: Visual Pattern Discrimination, *IRE Trans. Information Theory*, Febr. 1962, pp. 84-92.
2. HARALICK, R. M. - SHANMUGAM, K. - DINSTEN, I.: Textural Features for Image Classification, *IEEE Trans. Syst. Man Cybernet*, Vol. 3, Nov. 1973, pp. 610-621.
3. GALLOWAY, M. H.: Texture Analysis Using Gray Level Run Lengths, *Comput. Graphics. Image Process*, Vol. 4, 1975, pp. 172-179.
4. WU, CHUNG-MING - CHEN, YUNG-CHANG: Statistical Feature Matrix for Texture Analysis, *Graphical Models and Image Processing*, Vol. 54, No. 5, Sept. 1992, pp. 407-419.
5. HARALICK, R. M.: Statistical and Structural Approaches to Texture, *Proc. IEEE* 67, 1979, pp. 786-804.
6. MALLAT, S. G.: A Theory for Multiresolution Signal Decomposition: The Wavelet Representation, *IEEE Trans. Pattern Anal. Mach. Intelligence*, Vol. 11(7), July, 1989, pp. 674-693.
7. BURT, P. J. - ADELSON, E. H.: The Laplacian Pyramid as a Compact Image Code, *IEEE Trans. Commun*, Vol. Com-31, Apr. 1983, pp. 532-540.
8. DAUBECHIES, I.: Orthonormal Bases of Compactly Supported Wavelets, *Commun. Pure Appl. Math.*, Vol. 41, Nov. 1988, pp. 909-996.
9. CHETVERIKOV, D.: Textural Anisotropy Features for Texture Analysis, *Proc. IEEE Conf. on PRIP*, Dallas, 1981, pp. 583-588.
10. BASTIAANS, M.: Gabor's Expansion of a Signal into Gaussian Elementary Signals, *Proc. IEEE*, Vol. 68, April, 1980, pp. 538-539.
11. CHETVERIKOV, D.: Experiments in the Rotation-Invariant Texture Discrimination Using Anisotropy Features, *Proc. 6th ICPR*, Munich, 1982, pp. 1071-1073.
12. CHETVERIKOV, D.: GLDH Based Analysis of Texture Anisotropy and Symmetry: an Experimental Study, submitted to 12th ICPR, Jerusalem, 1994.
13. ALDROUBI, A. - UNSER, M.: Families of Wavelet Transforms in Connection with Shannon's Sampling Theory and Gabor Transform in Wavelets (ed. C. Chui), Acad. Press., 1992.
14. CHANG, T. - KUO, C.-C. J.: Texture Analysis and Classification and Tree-Structured Wavelet Transform, *IEEE Transactions on Image Processing*, Vol. 2, Oct. 1993, pp. 429-441.
15. KASS, M. - WITKIN, A.: Analyzing Oriented Patterns, *CVGIP* 37, 1987, pp. 362-385.
16. RAO, A. R. - SCHUNK, B. G.: Computing Oriented Texture Fields, *CVGIP: Graphical Models and Image Processing*, Vol. 53, 1991, pp. 157-185.
17. RAO, A. R. - JAIN, R.: Computerized Flow Fields Analysis: Oriented Texture Fields, *IEEE PAMI*, Vol. 14, 1992, pp. 693-709.

18. RAO, A. R. – LOHSE, G. L.: Identifying High Level Features of Texture Perception, *CVGIP: Graphical Models and Image Processing*, Vol. 55, 1993, pp. 218–233.
19. DENSLOW S. et. al.: Statistically Characterized Features for Directionality Quantitation in Patterns and Textures, *Pattern Recognition*, Vol. 26, 1993, pp. 1193–1205.
20. CONNERS, R. W. – HARLOW, C. A.: A Theoretical Comparison of Texture Algorithms, *IEEE Trans. PAMI*, Vol. 2, 1980, pp. 204–222.
21. WESZKA, J. et. al.: A Comparative Study of Texture Measures for Terrain Classification, *IEEE Trans. SMC*, Vol. 4, 1976, pp. 269–285.
22. DAVIS, L. S.: Polarograms: a New Tool for Image Texture Analysis, *Pattern Recognition*, Vol. 13, 1981, pp. 219–223.
23. LABONT, F. – SHAPIRA, Y. – COHEN, P.: A Perceptually Plausible Model for Global Symmetry Detection, *Proc. 4th ICCV*, Berlin, 1993, pp. 258–263.
24. ZABRODSKY, H. – PELEG, S.: Hierarchical Symmetry, *Proc. 11th ICPR C*, The Hague, 1992, pp. 9–12.
25. REISFELD, D. – WOLFSON, H. – YESHURUN, Y.: Detection of Interest Points by a Symmetry Operator, *Proc. 3rd ICCV*, Osaka, 1990.
26. BONNEH, Y. – REISFELD, D. – YESHURUN, Y. Texture Discrimination by Generalized Symmetry, *Proc. 4th ICCV*, Berlin, 1993, pp. 261–265.
27. CHETVERIKOV, D.: Generating Contrast Curves for Texture Regularity Analysis, *Pattern Recognition Letters*, Vol. 12, 1991, pp. 437–444.
28. CONNERS, R.W. – HARLOW, C. A.: Toward a Structural Texture Analyzer Based on Statistical Methods, *Computer Graphics and Image Processing*, Vol. 12, 1980, pp. 224–256.
29. MODESTINO, J.W. – FRIES, R. W. – VICKERS, A. L.: Texture Discrimination Based upon an Assumed Stochastic Texture Model, *IEEE Trans. Pattern Anal. Machine Intell.* Vol. 3, 1981, pp. 557–579.
30. PARKKINEN, J. – SELKAINAHO, K. – OJA, E.: Detecting Texture Periodicity from the Cooccurrence Matrix, *Pattern Recognition Letters*, Vol. 11, 1990, pp. 43–50.
31. ZHUANG, C. – DUNN, S.: The Amplitude Varying Statistical Approach for Texture Classification, *Pattern Recognition Letters*, Vol. 11, 1990, pp. 143–149.
32. ZUCKER, S. W. – TERZOPOULOS, D.: Finding Structure in Cooccurrence Matrices for Texture Analysis, *Computer Graphics and Image Processing*, Vol. 12, 1980, pp. 1286–1303.
33. JULESZ, B.: Experiments in the Visual Perception of Texture, *Scientific American*, Vol. 232, 1975, pp. 34–43.
34. KUNDU, A. – CHEN, JIA-LIN: Texture Classification Using QMF Bank-Based Sub-band Decomposition, *Graphical Models and Image Processing*, Vol. 54, Sept. 1992, pp. 369–384.
35. CHELAPPA, R. – CHATTERJEE, S.: Classification of Textures Using Gaussian Markov Random Fields, *IEEE Trans. Acoust. Speech Signal Process*, Vol. 34(4), Aug. 1983, pp. 959–963.
36. ORR, R. S.: The Order of Computation for Finite Discrete Gabor Transforms, *IEEE Trans. on Signal Processing*, Vol. 41, 1993, pp. 122–130.
37. EBRAHIMI, T. – KUNT, M.: Image Compression by Gabor Expansion, *Opt. Eng.*, Vol. 30, 1991, pp. 873–880.